Dynamic stability versus thermodynamic performance in a simple model for a Brownian motor

Moisés Santillán*
Centro de Investigación y Estudios Avanzados del IPN, Unidad Monterrey, Parque de Investigación e Innovación Tecnológica, 66600 Apodaca NL, Mexico

Michael C. Mackey†
Department of Physiology, Department of Physics, Department of Mathematics, and Centre for Nonlinear Dynamics, McGill University, 3655 Promenade Sir William Osler, Montréal, Québec, Canada H3G 1Y6

(Received 28 August 2008; published 19 December 2008)

Homeostasis allows living organisms to perform in optimal conditions despite ever-changing surroundings. Dynamically, it corresponds to a stable steady state, and so its quality can be judged by the volume of the corresponding basin of attraction and/or the length of the relaxation time. Motivated by the fact that the vast majority of intracellular processes involve enzymatic reactions and, as some people have suggested, models similar to those of Brownian motors can be used to study them, here we introduce a simple Brownian motor model and use it to gain insight into the relation between efficiency and stability properties previously observed in macroscopic systems. For this, we analyze the existence, uniqueness, and stability of the motor's steady state; study its thermodynamic process variables, their relation, and their dependence on the model parameters; and compare the Brownian motor relaxation time and thermodynamic properties. Finally, since the steady state is unique and globally stable, we discuss our results from the standpoint of the energetic costs of maintaining a homeostatic state with short relaxation times.

DOI: 10.1103/PhysRevE.78.061122 PACS number(s): 05.40.−a, 05.45.−a, 05.70.Ln

I. INTRODUCTION

In 1932 Cannon [1] introduced the concept of homeostasis, stating: "The coordinated physiological processes which maintain most of the steady states in the organism are so complex and so peculiar to living beings—involving, as they may, the brain and nerves, the heart, lungs, kidneys and spleen, all working cooperatively—that I have suggested a special designation for these states, homeostasis. The word does not imply something set and immobile, a stagnation. It means a condition—a condition which may vary, but which is relatively constant." Although a name did not exist for it at the time, Bernard had already discussed this concept around 1860: "The constancy of the internal environment is the condition for a free and independent life" [2]. Now homeostasis is regarded as a cornerstone concept in biology. It is found, to some extent, in all living beings, and allows them to perform in optimal conditions in spite of ever-changing surroundings and inputs.

From a dynamical point of view, homeostasis corresponds to the existence of a stable steady state [3–5]. Hence, the quality of homeostasis can be judged by the volume of the steady-state basin of attraction and/or the relaxation time with which the system returns to the steady state after a perturbation. Having a large basin of attraction is important because it allows the system to come back to the steady state even if it suffers large alterations. On the other hand, a rapid relaxation time permits the system to quickly recover its optimal state after a perturbation. Furthermore, the shorter the system relaxation time, the smaller the amplitude of the fluctuations in its state variables, caused by an ever-changing environment.

Previous work on finite-time thermodynamic engines [6,7], and on the stretch reflex regulatory pathway of muscle contraction [8], has shown that those systems' stability properties depend on the same parameters that determine their thermodynamic characteristics (power, efficiency, etc.). Indeed, a trade-off between efficiency and stability properties has been noted in these two cases, with respect to some parameters. If these results are more general and they apply to a wide range of intracellular energy-converting processes, it would mean that the maintenance of the cell homeostatic state entails an expenditure of energy, which has to be taken into consideration to understand how organisms adapt to a constantly changing environment.

The majority of intracellular energy-converting processes involve enzymatic biochemical reactions. Moreover, it has been suggested that the functioning of enzymes resembles that of Brownian motors in several aspects, and thus that models very similar to those of Brownian motors can be used to study enzymatic reactions [9–12]. These considerations indicate that Brownian motors are excellent candidates to carry out a case study aimed at gaining insight, at the molecular level, into the relation between efficiency and stability properties noted above. With these ideas in mind, in this paper we introduce a simple Brownian motor model; analyze the existence, uniqueness, and stability of the steady state; study the motor thermodynamic process variables, their relation to and their dependence on the model parameters; and compare the Brownian motor dynamic and thermodynamic properties. Finally, given that the model here studied possesses global stability, we discuss our results from the standpoint of the energetic costs of maintaining a homeostatic state with short relaxation times.

*msantillan@cinvestav.mx
†michael.mackey@mcgill.ca

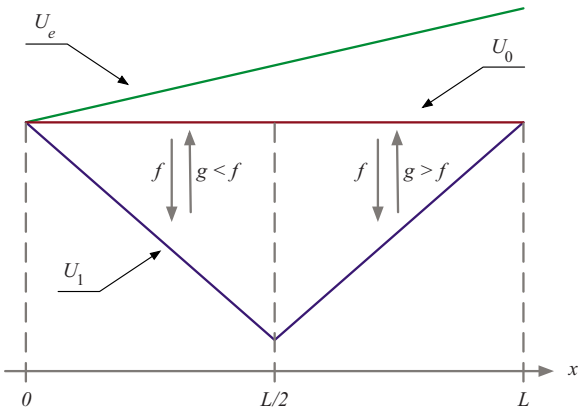

FIG. 1. (Color online) Schematic representation of the Brownian motor considered here. U_0 and U_1 represent the alternate potentials between which the molecule flips, while U_e is the external potential that acts upon the molecule at all times. Recall that a potential U and its corresponding force F are related by $F=-dU/dx$. f and g respectively represent the transition rates from U_0 to U_1 and from U_1 to U_0.

II. THEORY

Consider a Brownian motor—see Fig. 1—in which a molecule flips between potentials $U_0(x)$ and $U_1(x)$ with switching rates $f(x)$ from U_0 to U_1 and $g(x)$ from U_1 to U_0. Assume as well a constant external force $-F_e$ acting upon the Brownian molecule—the corresponding potential being $U_e=F_e x$. Let $\rho_0(x,t)dx$ and $\rho_1(x,t)dx$, respectively, denote the probabilities that the molecule is located in the interval $[x,x+dx]$ under the influence of potentials U_0 and U_1 at time t. The dynamics of $\rho_0(x,t)$ and $\rho_1(x,t)$ are described by the following set of Smoluchowsky equations [13]:

$$\frac{\partial \rho_0(x,t)}{\partial t} = \frac{\partial^2}{\partial x^2}[D_0(x)\rho_0(x,t)] - \frac{\partial}{\partial x}\left(\frac{F_0(x)-F_e}{\nu_0(x)}\rho_0(x,t)\right) - f(x)\rho_0(x,t) + g(x)\rho_1(x,t), \tag{1}$$

$$\frac{\partial \rho_1(x,t)}{\partial t} = \frac{\partial^2}{\partial x^2}[D_1(x)\rho_1(x,t)] - \frac{\partial}{\partial x}\left(\frac{F_1(x)-F_e}{\nu_1(x)}\rho_1(x,t)\right) + f(x)\rho_0(x,t) - g(x)\rho_1(x,t), \tag{2}$$

where $D_i(x)$ and $\nu_i(x)$ $(i=0,1)$ are the diffusion and the viscosity coefficients when the molecules are in a potential U_i, and

$$F_i = -\frac{dU_i}{dx} \tag{3}$$

is the corresponding force.

In the limit of large switching rates f and g (the transitions are rapid compared with the diffusion dynamics), the following quasi-steady-state approximation can be made [13]:

$$f(x)\rho_0(x,t) = g(x)\rho_1(x,t). \tag{4}$$

With this, the equation governing the dynamics of the probability distribution $\rho(x,t)=\rho_0(x,t)+\rho_1(x,t)$ is

$$\frac{\partial \rho(x,t)}{\partial t} = -\frac{\partial J(x,t)}{\partial x}, \tag{5}$$

where

$$J(x,t) = -\frac{\partial}{\partial x}[D(x)\rho(x,t)] + \frac{F(x)-\tilde{F}_e}{\nu(x)}\rho(x,t) \tag{6}$$

is the probability current, and

$$D(x) = \frac{D_0(x)g(x)+D_1(x)f(x)}{g(x)+f(x)}, \tag{7}$$

$$\frac{1}{\nu(x)} = \frac{\nu_0(x)+\nu_1(x)}{2\nu_0(x)\nu_1(x)}, \tag{8}$$

$$F(x) = F_0(x)\frac{g(x)}{g(x)+f(x)}\frac{2\nu_1(x)}{\nu_0(x)+\nu_1(x)} + F_1(x)\frac{f(x)}{g(x)+f(x)}\frac{2\nu_0(x)}{\nu_0(x)+\nu_1(x)}, \tag{9}$$

$$\tilde{F}_e(x) = 2F_e\frac{\nu_1(x)g(x)+\nu_0(x)f(x)}{[\nu_0(x)+\nu_1(x)][f(x)+g(x)]}. \tag{10}$$

Assume for the sake of simplicity that $D_1(x)$ and $D_2(x)$ are constant and equal to each other, as are $\nu_0(x)$ and $\nu_1(x)$. This implies [see Eqs. (7)–(10)] that

$$D = D_1 = D_2, \quad \nu = \nu_1 = \nu_2,$$

$$F(x) = \frac{F_0(x)g(x)+F_1(x)f(x)}{f(x)+g(x)}, \quad \tilde{F}_e(x) = F_e. \tag{11}$$

We see from Eq. (5) that the current J is constant in the steady state. Furthermore, following [14], the general steady-state solution of Eq. (5), with the simplifying assumptions in (11), is

$$\rho_*(x) = \frac{e^{-\phi(x)}}{Z} - \frac{J}{D}e^{-\phi(x)}\int_0^x e^{\phi(x')}dx', \tag{12}$$

where

$$\phi(x) = -\frac{1}{D\nu}\int_0^x [F(x')-F_e]dx', \tag{13}$$

while Z and J are constants to be determined from the normalization and boundary conditions imposed on the probability density. In particular, if the potentials $U_i(x)$ $(i=0,1)$ are periodic, with spatial period L, the normalization and boundary conditions are

$$\int_0^L \rho_*(x)dx = 1 \quad \text{and} \quad \rho_*(0) = \rho_*(L), \tag{14}$$

respectively. Equations (12) and (14) further imply that

$$0 = \rho_*(L) - \rho_*(0) = \frac{e^{-\phi(L)} - e^{-\phi(0)}}{Z} - \frac{J}{D} e^{-\phi(L)} \int_0^L e^{\phi(x')} dx'. \tag{15}$$

Hence, the potential $\phi(x)$ must be nonperiodic in order for the steady-state current J to be nonzero. If this is the case, we have from Eq. (15) that

$$Z = \frac{D}{JL} \frac{e^{-\phi(L)} - e^{-\phi(0)}}{e^{-\phi(L)}} \left(\int_0^1 e^{\phi(L\zeta)} d\zeta \right)^{-1}, \tag{16}$$

with $\zeta = x/L$. Finally, by substituting (16) into (12) and normalizing the density, we obtain

$$J = \frac{D}{L^2} \left(\frac{e^{-\phi(L)}}{e^{-\phi(L)} - e^{-\phi(0)}} \int_0^1 e^{-\phi(L\zeta)} d\zeta \int_0^1 e^{\phi(L\zeta)} d\zeta - \int_0^1 e^{-\phi(L\zeta)} \int_0^\zeta e^{\phi(L\zeta')} d\zeta' d\zeta \right)^{-1} \tag{17}$$

for the probability current.

It is a direct consequence from [15] (see also [16], Sec. IV) that, for the assumptions we have made, the steady-state solution ρ_* in (12) is globally asymptotically stable in the sense that every initial ρ_{init} will converge to ρ_* in L^1 norm.

The rate of approach of a nonequilibrium $\rho(x,t)$ to the steady-state solution $\rho_*(x)$ can be estimated as follows. Let $\rho_*(x)$ be the steady-state solution of (5), and consider another solution $\rho(x,t)$ written as

$$\rho(x,t) = \rho_*(x) + \delta(x,t). \tag{18}$$

From (18) and the fact that ρ and ρ_* are both solutions of Eq. (5), it follows that δ satisfies the Fokker-Planck equation

$$\frac{\partial \delta(x,t)}{\partial t} = D \frac{\partial^2 \delta(x,t)}{\partial x^2} - \frac{\partial}{\partial x} \left(\frac{F(x) - F_e}{\nu} \delta(x,t) \right).$$

Assume that $\delta(x,t) = e^{\lambda t} \psi(x)$; then $\psi(x)$ and λ satisfy the eigenvalue equation

$$\lambda \psi(x) = D \frac{\partial^2 \psi(x)}{\partial x^2} - \frac{\partial}{\partial x} \left(\frac{F(x) - F_e}{\nu} \psi(x) \right). \tag{19}$$

The eigenvalues of the Fokker-Planck operator determine the stability of the steady-state solution of (5). Since we know that ρ_* is globally stable, then all of the eigenvalues must satisfy $\lambda_n \leqslant 0$. It follows from a comparison of Eqs. (5) and (19), with D and ν constant, that the eigenfunction associated with the null eigenvalue corresponds to the steady-state solution of (5). A relaxation time τ_n can thus be defined for every nonzero eigenvalue λ_n as

$$\tau_n = -\frac{1}{\lambda_n}. \tag{20}$$

Finally, the largest nonzero eigenvalue—which is the one with the smallest absolute value—dominates the long-term dynamics of $\rho(x,t)$ as it approaches the steady-state solution $\rho_*(x)$.

Following Qian [13], thermodynamic steady-state process variables can be defined for a Brownian motor as follows. The average energy rate that a molecule, moving in the effective potential $\phi(x)$, obtains from the potentials U_0 and U_1 is

$$\mathcal{E} = \int_0^L F(x) J(x) dx. \tag{21}$$

Similarly, the power exerted against the external force can be calculated as

$$\mathcal{P} = \int_0^L F_e(x) J(x) dx. \tag{22}$$

From Eqs. (21) and (22) and the first law of thermodynamics, the heat production rate is

$$\mathcal{Q} = \mathcal{E} - \mathcal{P}. \tag{23}$$

Finally, the efficiency of energy conversion is

$$\eta = \frac{\mathcal{P}}{\mathcal{E}}. \tag{24}$$

If we assume that F_e is constant and that the Brownian motor is in a steady state, then (21) and (22) become

$$\mathcal{E} = J \int_0^L F(x) dx \tag{25}$$

and

$$\mathcal{P} = J F_e L. \tag{26}$$

III. MODEL DEVELOPMENT AND RESULTS

Define the forces F_e, $F_0(x)$, and $F_1(x)$ by

$$F_e = \frac{D \nu V_e}{L}, \quad F_0 = 0, \quad F_1 = \begin{cases} 2D\nu V/L, & 0 \leqslant x \leqslant L/2, \\ -2D\nu V/L, & L/2 \leqslant x \leqslant L. \end{cases} \tag{27}$$

Let $\varepsilon(x)$ be given by

$$\varepsilon(x) = \frac{f(x)}{f(x) + g(x)} = \begin{cases} a, & 0 \leqslant x \leqslant L/2, \\ b, & L/2 \leqslant x \leqslant L, \end{cases} \tag{28}$$

and assume that $0 \leqslant b \leqslant 1/2 \leqslant a < 1$. That is, $f > g$ if $x < L/2$, and $g > f$ otherwise. A schematic representation of the resulting model is pictured in Fig. 1.

We have from (11), (27), and (28) that

$$F(x) = \varepsilon(x) F_1(x). \tag{29}$$

Furthermore, it follows from Eqs. (13), (27), and (29) that the normalized potential $\phi(x)$ takes the form

$$\phi(x) = \begin{cases} -(aV - V_e/2)2x/L & \text{if } 0 \leqslant x \leqslant L/2, \\ -(aV - V_e/2) + (bV + V_e/2)(2x/L - 1) & \text{if } L/2 \leqslant x \leqslant L. \end{cases} \tag{30}$$

In Fig. 2 the potential ϕ is plotted as a function of x. After substituting this expression for ϕ into (17), the probability current becomes

$$J = \frac{4D}{L^2}\left[\frac{e^{-2B}}{e^{A-B}-1}\left(\frac{e^A-1}{A}+\frac{e^B-1}{B}\right)\left(e^A\frac{e^B-1}{B}+e^B\frac{e^A-1}{A}\right) - \frac{1}{A}\left(\frac{e^A-1}{A}-1\right) - \frac{1}{B}\left(1-\frac{1-e^{-B}}{B}\right) - \frac{e^A-1}{A}\cdot\frac{1-e^{-B}}{B}\right]^{-1}, \tag{31}$$

where $A = aV - V_e/2$ and $B = bV + V_e/2$.

From (21), (22), (24), and (30), the average rate of energy input, power output, and efficiency of this model are

$$\mathcal{E} = \frac{3}{4}D\nu V J(V, V_e), \quad \mathcal{P} = \frac{1}{2}D\nu V_e J(V, V_e), \quad \eta = \frac{2}{3}\frac{V_e}{V}, \tag{32}$$

where $J(V, V_e)$ is given by (31). We can use (31) and (32) to analyze the model steady-state thermodynamic behavior. To reduce the number of parameters, consider the case $a=1$ and $b=0$. That is, $A = V - V_e/2$ and $B = V_e/2$. The resulting current J is plotted vs V_e in Fig. 3 for different values of V. Notice that, in all cases, J decreases monotonically with V_e, the probability current J vanishes when $V_e = V$, and the curves J vs V_e are concave. The maximum J value, $J^*(V) = J(V, V_e = 0)$, increases together with V, as well as the concavity of the J vs V_e curves. The graph of $J^*(V)$ vs V is shown in Fig. 4. Note that J^* increases monotonically as the depth (V) of the potential U_1 increases.

The dependence on V and V_e of the power ($\mathcal{P}$) exerted by the Brownian motor against the external force $-F_e$ is shown in Fig. 5. There, $\mathcal{P}$ is plotted vs V_e for different values of V. In all cases, $\mathcal{P}$ is zero at $V_e = 0$ and $V_e = V$, and the $\mathcal{P}$ vs V_e curves are convex with a single maximum. The value of V_e that maximizes $\mathcal{P}$ decreases as V increases, while the maximum $\mathcal{P}$ value ($\mathcal{P}^*$) increases monotonically with V, as also shown in Fig. 6. Interestingly, the $\mathcal{P}^*$ vs V_e curves resulting from this model behave similarly to those reported in analogous studies on Brownian motors [17,18]

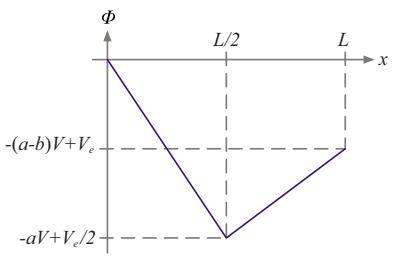

FIG. 2. (Color online) Normalized potential ϕ, as given by Eq. (30), vs x.

Finally, as seen in (32), the Brownian motor efficiency η varies linearly with V_e. In particular $\eta(V_e = 0) = 0$ and $\eta(V_e = V) = 2/3$.

Let $\psi(x)$ be one eigenfunction of the Fokker-Planck operator in Eq. (19) and λ its corresponding eigenvalue. Following [9,10,14], Eq. (19) can be transformed into the Schrödinger-like equation

$$\frac{\partial^2 \xi(x)}{\partial x^2} - V_S(x)\xi(x) = \frac{\lambda}{D}\xi(x), \tag{33}$$

via the change of variable

$$\xi(x) = \psi(x)e^{\phi(x)/2},$$

with $\phi(x)$ as defined in Eq. (13), and

$$V_S(x) = \left(\frac{1}{2}\frac{\partial\phi(x)}{\partial x}\right)^2 - \frac{1}{2}\frac{\partial^2\phi(x)}{\partial x^2}. \tag{34}$$

Substitution of (30) into (34) yields

$$V_S(x) = \begin{cases} (A/L)^2, & 0 \leqslant x \leqslant L/2, \\ (B/L)^2, & L/2 \leqslant x \leqslant L. \end{cases} \tag{35}$$

Assume that the solution of (33) takes the form

$$\xi(x) = \begin{cases} -\alpha_a \cos(\omega_a x) + \beta_a \sin(\omega_a x), & 0 \leqslant x \leqslant L/2, \\ -\alpha_b \cos(\omega_b x) + \beta_b \sin(\omega_b x), & L/2 \leqslant x \leqslant L. \end{cases} \tag{36}$$

Substitution of (35) and (36) into (33) leads to the conclusion that $\xi(x)$ must satisfy the equations

$$-\omega_a^2\xi(x) - (A/L)^2\xi(x) = (\lambda/D)\xi(x) \quad \text{if } 0 \leqslant x \leqslant L/2,$$

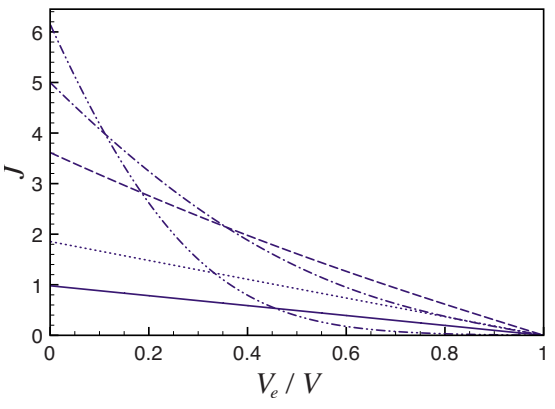

FIG. 3. (Color online) J (in units of D/L^2) vs V_e (normalized to V) for various values of V. The line patterns are as follows: – $V = 1D\nu$, ⋯ $V = 2D\nu$, – – $V = 5D\nu$, –·– $V = 10D\nu$, and –··– $V = 20D\nu$.

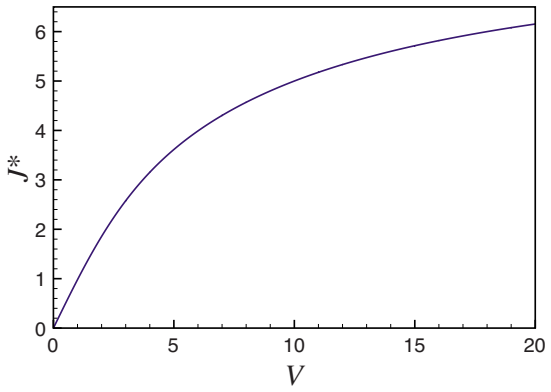

FIG. 4. (Color online) Maximal current value J^* (in units of D/L^2) vs V.

$$-\omega_b^2\xi(x) - (B/L)^2\xi(x) = (\lambda/D)\xi(x) \quad \text{if } L/2 \leqslant x \leqslant L,$$

where λ is an eigenvalue of the Fokker-Planck operator defined in (19), and λ/D is an eigenvalue of the Schrödinger-like equation (33). These equations further imply that

$$-\lambda = D[\omega_a^2 + (A/L)^2] = D[\omega_b^2 + (B/L)^2].$$

Moreover, since $A=V-V_e$ and $B=V_e$,

$$-\lambda \geqslant \frac{D}{L^2}(V-V_e)^2, \tag{37}$$

whenever $0 \leqslant V_e \leqslant V$. Equation (37) provides an upper bound for the eigenvalues λ_n of the Fokker-Planck operator in Eq. (19), and is consistent with the fact that the steady state is globally stable ($\lambda_n < 0, \forall n$). Finally, from (20) and (37), an upper bound can be calculated for the relaxation times that govern the return of the system to the steady state after a perturbation:

$$\tau \leqslant \frac{L^2}{D(V-V_e)^2}. \tag{38}$$

Given that, of all the relaxation times, the largest one dominates the system dynamics as it approaches to the steady

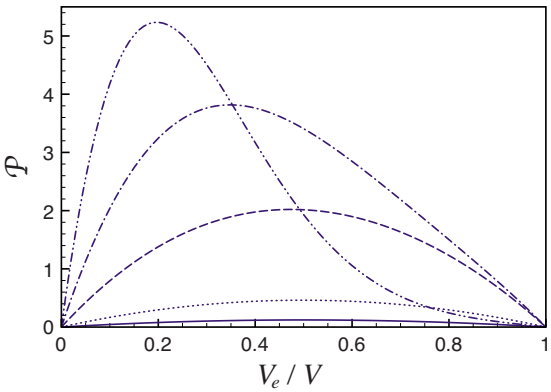

FIG. 5. (Color online) Plots of $\mathcal{P}$ (in units of $D^2\nu/L^2$) vs V_e (normalized to V) for various values of V. The line patterns are as follows: – $V=1D\nu$, ⋯ $V=2D\nu$, – – $V=5D\nu$, –·– $V=10D\nu$, and –··– $V=20D\nu$.

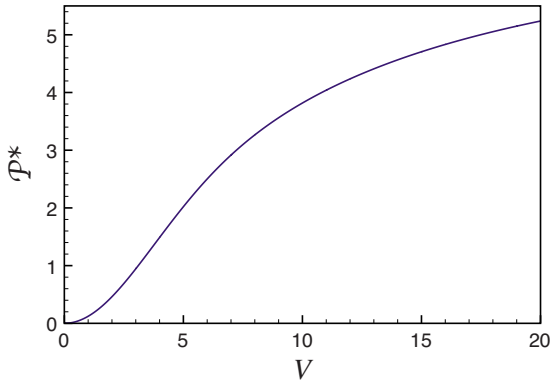

FIG. 6. (Color online) Maximal power output value $\mathcal{P}^*$ (in units of $D^2\nu/L^2$) vs V.

state, the upper bound provided by (38) is an estimation of how rapidly the steady state is approached. The smaller the value of the right-hand side of Eq. (38), the more rapid the approach to the steady state. Bier *et al.* [19] extensively studied the relaxation time on a potential slope back to a Boltzmann distribution, starting from a Dirac δ distribution centered at the point of interest. In agreement with our results, they found that the relaxation time is inversely proportional to the square of the potential depth.

IV. DISCUSSION AND CONCLUSIONS

In this paper we have used a simple Brownian motor model to gain insight into the relation between stability (relaxation time) and thermodynamic (power, efficiency, etc.), properties commonly observed in energy-converting systems. We will discuss our results in this section from the standpoint of the energetic costs concomitant with the maintenance of a short relaxation time and its consequences for cellular homeostasis.

The model introduced here considers a diffusing overdamped molecule that flips between two periodic symmetric potentials U_0 and U_1, while subjected to a constant external force $-F_e$. The potential U_0 is constant and equal to zero, which means that the molecule diffuses freely under its influence. Conversely, the potential U_1 is piecewise linear, concave, and has a single minimum at $x=L/2$, where L is the potential spatial period. Thus, under the influence of U_1, the molecule tends to fluctuate around the point of minimum potential. This setup is commonly thought to be the underlying mechanism for motor protein motion, and it has been suggested that similar models can be used to study enzyme function [9–12].

In the present model, flux results from varying the transition rates between potentials U_0 and U_1 along the x axis (see Fig. 1) which is also how isotropy is broken. These systems have been termed "feedback control ratchets" by Cao *et al.* [20], and transport in them was derived and studied by Ciudad *et al.* [21]. Indeed, by taking $a=1$ and $b=0$ in Eq. (28), we go to the case studied in Ref. [21]. This assumption means that, whenever the Brownian molecule is under the influence of U_0 and $0 \leqslant x \leqslant 1/2$, it immediately flips to U_1

and remains there, diffusing to $x \approx 1/2$, whereas, if $1/2 < x \leqslant 1$ and the molecule is under the influence of U_1, it rapidly flips to U_0 and remains there, diffusing freely.

The fact that this model is analytically solvable allows a complete analysis, using standard techniques, of its thermodynamic characteristics (power, efficiency, etc.) and of its steady-state stability. In particular, we have proven that our model has a unique globally stable steady state. Therefore, we focus the forthcoming discussion on the system relaxation time, which determines the drive-away dynamics of the Brownian motor and, as discussed in the Introduction, needs to be short to preserve cellular homeostasis.

From Eq. (31), the probability current is determined by D, L, V, and V_e. In particular,

$$J \propto \frac{D}{L^2}$$

when V_e and V are fixed. The dependence of J on V_e and V can be analyzed from Fig. 3. Notice that (for fixed values of D, L, and V) J decreases monotonically as V_e increases and is zero at $V_e = V$. Furthermore, the J vs V_e curves are concave, and their concavity increases together with the value of V. Finally, the maximum J value, reached at $V_e = 0$, is an increasing function of V (cf. Fig. 4).

The average speed of a molecule moving under the influence of the external force $-F_e$ and the potentials U_0 and U_1 is $v = JL$ [13]. Therefore, we can conclude from the considerations in the previous paragraph that v decreases as the absolute value of the external force, F_e, increases ($F_e \propto V_e$), that the maximum speed is reached at $F_e = 0$ and is a growing function of the depth (V) of the potential U_1, and that v is proportional to D/L.

For the power $\mathcal{P}$ exerted by the Brownian motor against the external force ($-F_e$), it follows from (31) and (32) that it is proportional to $D^2\nu/L^2$. Furthermore, $\mathcal{P}$ also depends on V_e and V. The curves $\mathcal{P}$ vs V_e are convex with a single maximum, $\mathcal{P}$ is zero at $V_e = 0$ and $V_e = V$, the V_e value that maximizes $\mathcal{P}$ is close to $V/2$ when $V \approx 0$ and decreases as V increases, and the maximum $\mathcal{P}$ value increases with V.

From these observations it is clear that both the velocity v and the power $\mathcal{P}$ can be enhanced by increasing the diffusion coefficient D and/or decreasing the spatial period L. From Eq. (38) the relaxation-time upper bound τ increases with L and decreases with D. Thus the parameters D and L have a similar effect on the Brownian motor thermodynamic properties (v and P) and the relaxation time associated with its steady state. Increasing D and/or decreasing L make the power and the velocity increase and increase the rapidity with which the steady state is approached.

The Brownian motor velocity v (31), power output $\mathcal{P}$ (32), efficiency η (32), and relaxation-time upper bound τ (38) depend on both V_e and V. When V is kept constant, increases in V_e lead to decreases in v (see Fig. 3 and remember that $v \propto J$) and to increases in η and τ (indeed $\tau \to \infty$ as $V_e \to V$). In contrast, the curves $\mathcal{P}$ vs V_e are convex with a single maximum, and the V_e value that maximizes $\mathcal{P}$ decreases as V increases. Thus, if V is high enough, a regime can be found where the system has a high power output, its steady state has a short relaxation time, and has a high velocity. Nonetheless, since V_e is necessarily small in this regime, the efficiency of energy conversion is also small.

It is interesting to analyze how the properties of the Brownian motor depend on the value of the parameter V. In Fig. 4, the maximum current value $J^*(V) = J(V, V_e = 0)$ is plotted vs V, and J^* is a monotonically increasing function of V. Since $v = JL$, the maximum speed is also an increasing function of the depth (V) of the potential U_1. We have seen that the curve $\mathcal{P}$ vs V_e is zero at $V_e = 0$ and $V_e = V$, and that it has a single maximum $\mathcal{P}^*$ at an intermediate V_e value. Notice from Fig. 6 that $\mathcal{P}^*$ increases together with V. Furthermore, from (38) the minimum value of the relaxation-time upper bound decreases as V increases. That is, larger V values imply a more rapid approach to the steady state. Finally, in this model, the maximum possible efficiency is always $2/3$, regardless of the V value (32). To conclude, as the thermodynamic properties (v and $\mathcal{P}$) improve, the steady-state relaxation time decreases, and the efficiency remains unaffected as V increases.

In summary, after analyzing the effects of all the model parameters on the relaxation time of the system steady state as well as on thermodynamic properties like the system velocity, power, and efficiency, we find that every parameter affects both the system dynamics and thermodynamic characteristics. We conclude that all the parameters have a similar effect on the velocity, the power output, and the system relaxation time such that when the first two quantities increase, the last one decreases. With respect to the efficiency, the parameters can be classified into those that affect the efficiency, and those that do not. In the cases where the efficiency is affected, we noticed that it always increases when the power and the velocity decrease, and vice versa. The trade-off found between power and efficiency could be predicted beforehand because it has been observed in all kinds of energy-converting systems, both biological and artificial. More original is the fact that we found parameters that affect both the systems' relaxation time and its thermodynamic performance, some of which have to be tuned to reach a good compromise between those characteristics.

The trade-off observed between the system efficiency and the rapidity with which it returns to the steady state after a perturbation is particularly relevant from a biological viewpoint. All living cells have a finite availability of energy, which has to be distributed among the different energy consuming cellular activities. Improvement of one of such process necessarily has a deleterious effect on the others. This may explain why all organisms have reached an optimal compromise among their energy-consuming tasks. The results of the present work suggest that the system stability properties—in particular the relaxation time—need to be taken into account in this equation as well. In agreement with previous studies on macroscopic systems [6–8], our results suggest that decreasing the relaxation time of a cellular process has a negative effect on its efficiency, and therefore involves an energetic cost. If, as suggested by some authors [9–12], mathematical models similar to those for Brownian motors can be used to model enzymatic reactions and, as we suspect, the present results are more general than the context in which we have derived them, then the maintenance of the cell homeostatic state entails an expenditure of energy, which

has to be taken into consideration to understand how organisms adapt to a constantly changing environment.

ACKNOWLEDGMENTS

The authors thank Hong Qian and Andrew C. Fowler for their helpful advice, as well as the anonymous referees for their criticisms and suggestions. This work was partially done while both authors were visiting the Mathematical Institute at the University of Oxford, and was partially financed by CONACyT, México under Grant No. 55228, by the Natural Sciences and Engineering Research Council, Canada (NSERC) Grant No. OGP-0036920, Canada, and by MITACS.

[1] W. Cannon, *The Wisdom of the Body* (W. W. Norton and Company, New York, 1932).
[2] F. L. Holmes, Hist. Philos. Life Sci. **8**, 3 (1986).
[3] H. Kitano, Nat. Rev. Genet. **5**, 826 (2004).
[4] H. Kitano, Mol. Syst. Biol. **3**, 137 (2007).
[5] A. Lesne, Biol. Rev. Cambridge Philos. Soc. **83**, 509 (2008).
[6] M. Santillán, G. Maya, and F. Angulo-Brown, J. Phys. D **34**, 2068 (2001).
[7] R. Páez-Hernández, F. Angulo-Brown, and M. Santillán, J. Non-Equilib. Thermodyn. **31**, 173 (2006).
[8] R. Páez-Hernández and M. Santillán, Physica A **387**, 3574 (2008).
[9] M. Kurzyński, J. Chem. Phys. **101**, 255 (1994).
[10] M. Kurzyński, Biophys. Chem. **65**, 1 (1997).
[11] M. Garcia-Viloca, J. Gao, M. Karplus, and D. G. Truhlar, Science **303**, 186 (2004).
[12] X. S. Min, W. Xie, and B. Bagchi, J. Phys. Chem. B **112**, 454 (2008).
[13] H. Qian, J. Math. Chem. **27**, 219 (2000).
[14] H. Risken, *The Fokker-Planck Equation: Methods of Solution and Applications* (Springer, New York, 1984).
[15] K. Pichór and R. Rudnicki, J. Math. Anal. Appl. **215**, 56 (1997).
[16] M. C. Mackey and M. Tyran-Kamińska, Physica A **365**, 360 (2006).
[17] Y. Zhang, B. H. Lin, and J. C. Chen, Eur. Phys. J. B **53**, 481 (2006).
[18] M. Feito and F. J. Cao, Eur. Phys. J. B **59**, 63 (2007).
[19] M. Bier, I. Derényi, M. Kostur, and R. D. Astumian, Phys. Rev. E **59**, 6422 (1999).
[20] F. J. Cao, L. Dinis, and J. M. R. Parrondo, Phys. Rev. Lett. **93**, 040603 (2004).
[21] A. Ciudad, A. M. Lacasta, and J. M. Sancho, Phys. Rev. E **72**, 031918 (2005).